NMR Characterization of Elastomers Reinforced with in Situ Precipitated Silica

Leoncio Garrido,*,† James E. Mark,‡ Chen C. Sun,‡ Jerome L. Ackerman,† and Chen Chang†

NMR Center, Massachusetts General Hospital, 149 13th Street, Charlestown, Massachusetts 02129, and Department of Chemistry and The Polymer Research Center, University of Cincinnati, Cincinnati, Ohio 45221

Received September 11, 1990; Revised Manuscript Received February 19, 1991

ABSTRACT: Poly(dimethylsiloxane) (PDMS) model networks were reinforced by in situ precipitated silica following the usual sol–gel methods. Relatively large sample size and short reaction times were chosen to increase the probability of observing inhomogeneities. These elastomers were characterized by ^1H and ^{29}Si magic-angle spinning (MAS) NMR spectroscopy and ^1H NMR two-dimensional Fourier transform (2DFT) spin-echo imaging techniques. Bulk spin–lattice (T_1) and spin–spin (T_2) relaxation times were measured for all samples. The specific gravity of small pieces from regions of interest in selected specimens was measured. Only a small fraction (~5%) of the total protons present in the sample is visible in the NMR imaging experiments. The proton density and T_2 maps show clear and significant variations of NMR signal intensity throughout the sample due to the nonuniform hydrolysis of the tetraethylorthosilicate (TEOS) in the rubber. Under these precipitation conditions, silica precipitates mainly in the sample periphery as indicated by the proton density images, specific gravity, and ^{29}Si MAS NMR results. These studies indicate the importance of mass transport phenomena and the use of nondestructive test methods such as NMR imaging in the production of bulk specimens of in situ precipitated materials.

Introduction

The reinforcement of elastomers by blending with inorganic fillers (e.g., carbon black, silica) prior to the cross-linking reaction has been the method commonly used to produce tough elastomers of commercial interest.[1-3] Perhaps one of the most relevant examples is silicone (poly(dimethylsiloxane) or PDMS) rubber. In many of its applications, PDMS is filled with finely divided silicas in order to improve its mechanical properties (elastic modulus and tensile strength)[2] and physicochemical properties such as swelling resistance.

The reinforcement effect of fillers is often reduced by the presence of inhomogeneities in the elastomers, mainly due to a nonuniform dispersion of particles throughout the polymer matrix with formation of agglomerates.

Recently, the feasibility of precipitating silica into PDMS[4-8] and other polymers[9,10] by the catalyzed hydrolysis of an alkoxysilane or silicate has been demonstrated. The process involves the polymerization and branching by cocondensation of previously hydrolyzed silicate units as described by the following set of reactions:

hydrolysis

$$Si(OR)_4 + H_2O \xrightleftharpoons{H^+} (RO)_3SiOH + ROH$$

$$(RO)_3SiOH + H_2O \xrightleftharpoons{H^+} (RO)_2Si(OH)_2 + ROH$$

$$\vdots$$

cocondensation

$$2(RO)_3SiOH \xrightleftharpoons{H^+} (RO)_3SiOSi(OR)_3 + H_2O$$

$$\vdots$$

with R = $-CH_2CH_3$, to finally form a complicated silica network as shown in Figure 1.

Although the reinforcement mechanisms are not completely understood, a significant improvement in the mechanical properties of the polymers is observed, at least for relatively small and thin samples. Additionally, it has been shown that the filler particles generated by this procedure are generally unagglomerated and are very uniform in distribution and size, with diameters ranging from 150 to 250 Å.[5,11]

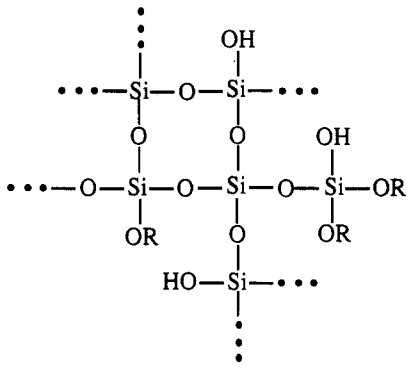

Figure 1. Sketch of the silica network formed by the catalyzed hydrolysis and cocondensation of tetraethylorthosilicate (TEOS) in aqueous media. The R groups represent $-CH_2CH_3$. The poly(dimethylsiloxane) chains interpenetrate the silica network (not shown for clarity).

As the specimen size increases, it might be expected that less uniform size and spatial distributions of particles throughout the specimen volume would be obtained. Because of the complexity of the chemistry involved in the hydrolysis process and the three-dimensional structure of the polymer network, it is very difficult to characterize these elastomers by using techniques conventionally applied to polymers or inorganic compounds. Nuclear magnetic resonance (NMR) spectroscopy, however, is very sensitive to the chemical composition and the molecular structure of a substance. These properties are reflected in the chemical shift spectrum as well as in the NMR relaxation parameters. NMR imaging techniques,[12-24] by producing visual pictures of the spatial variation of selected NMR properties, offer the possibility of selectively mapping the distribution of particular chemical species in a region of interest. Moreover, NMR imaging can also provide spatial information about changes in NMR

† Massachusetts General Hospital.
‡ University of Cincinnati.

0024-9297/91/2224-4067$02.50/0

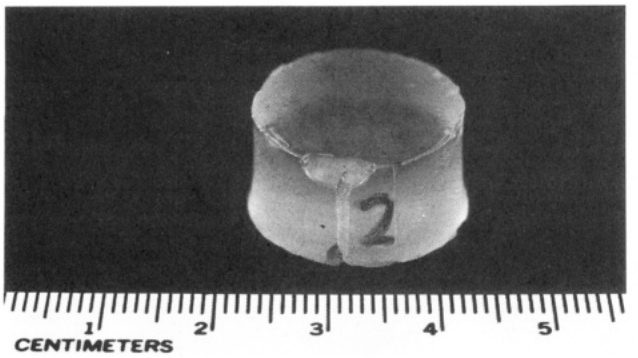

Figure 2. Poly(dimethylsiloxane) (PDMS) model network sample after TEOS hydrolysis for 90 min. The longitudinal mark on the side is for reference.

properties that can be correlated with alterations in molecular structure and dynamics.

The aim of this work is to develop NMR imaging techniques for the characterization of sol–gel-prepared organic–inorganic composites by mapping the organic phase distribution and the degree of alkoxide hydrolysis. In particular, we report the results obtained on PDMS model networks reinforced by in situ precipitated silica. We have obtained ^1H NMR images of the elastomers. In these images the variations in NMR signal intensity between different regions in the sample (image contrast) are a function of proton density and spin–spin (T_2) relaxation times. Such maps of NMR parameters provide a measure of the molecular mobility, which can in turn be related to the spatial variation of the relationship between the polymer and the filler throughout the specimen. To confirm the conclusions of the nondestructive imaging experiments, we have used ^1H and ^{29}Si magic-angle spinning (MAS) spectroscopy and density measurements to obtain information about the chemical composition of specific regions physically cut from the samples.

Experimental Part

PDMS model networks were prepared by an end-linking reaction of dihydroxyl-terminated PDMS chains having a number-average molecular weight, M_n, of 4200 with tetraethylorthosilicate (TEOS) in the usual manner.[25] The networks obtained, cylindrical pieces 20 mm in diameter and 9 mm in height (see Figure 2), were swollen to equilibrium in TEOS (which corresponds to a volume fraction of polymer of 0.70). Each swollen sample was then immersed in an aqueous solution of CF_3COOH at 5% w/w for 15–120 min. The acidic catalyst was chosen because of its high efficiency in hydrolyzing TEOS.[6] The samples were dried under vacuum to constant weight. The increase in dry weight gave the amount of SiO_2 precipitated within the sample in the elapsed time (see Table I). The large sample size and the short hydrolysis time assure inhomogeneous specimens.

The NMR experiments were performed in a Bruker MSL 400 spectrometer/imager equipped with an Oxford 9.4-T (^1H and ^{29}Si resonance frequencies of 400.13 and 79.48 MHz, respectively), 8.9-cm vertical-bore superconducting magnet. For ^1H NMR imaging, the radio-frequency (RF) coil used was a saddle type with a diameter of 25 mm and its longitudinal axis parallel to the static magnetic field. The pulsed-gradient amplitudes in the imaging experiments varied between 4 and 40 G cm^{-1}.

Bulk ^1H NMR T_1 and T_2 measurements were carried out by using inversion recovery (IR) and Hahn spin-echo sequences, respectively. The results are shown in Table I. The inversion time in the IR sequence was varied between 0 and 10 s. The echo time (TE, time between the 90° RF pulse and the center of the echo) in the spin-echo sequence ranged from 0.2 to 300 ms. The repetition time, TR, was 10 s in both cases, more than 5 times T_1.

^1H NMR images of the reinforced networks were obtained by using two-dimensional Fourier transform (2DFT) spin-echo techniques with TEs on the order of 3–25 ms. The selective excitation of a slice throughout the sample 500 μm thick was achieved with a 1-ms-wide sinc-function amplitude-modulated RF pulse. The pulse sequence TR was typically 3 s, and the total imaging time was 26 min. The digital resolution was $128X$ by $128Y$ pixels of 185 μm in both axes.

Solid-state ^1H and ^{29}Si MAS NMR spectra were acquired at ambient temperature by using a Bruker broad-band MAS probe. After the imaging experiments, three samples were selected and each one was divided into three regions (surface, intermediate, and center), as shown in Figure 3, and cut into small pieces. Then, they were ground and packed in zirconia rotors and spun at 4–6 kHz. The 90° pulses were 4–7 μs in length for ^{29}Si and ^1H NMR. The sequence employed was a single read pulse (tip angle 45° or less) followed by acquisition and relaxation recycle delay. All free induction decays were subjected to standard Fourier transformation and phasing. The chemical shifts were referenced to tetramethylsilane (TMS).

A slice of material was cut from the sample at the approximate imaging plane position. The density of pieces from the slice was measured using the Archimedes method employing mixtures of water/methanol or water/sodium chloride aqueous solution as the buoyant fluid.

Table I
Amount of Silica and T_1 and T_2 Values of Reinforced PDMS Model Networks[a]

sample ref	hydrolysis time, min	SiO_2, % w/w	T_1, s	T_{2S},[b] ms	f_S[c]	T_{2L},[d] ms
1	15	1.9	1.24	0.79 (0.02)	0.962 (0.006)	221 (135)
2	30	2.4	1.21	0.84 (0.02)	0.967 (0.007)	114 (81)
3	45	4.2	1.23	0.82 (0.02)	0.966 (0.008)	52 (34)
4	60	4.6	1.21	0.81 (0.02)	0.970 (0.007)	74 (54)
5	90		1.19	0.86 (0.03)	0.965 (0.008)	69 (46)
6	120	4.7	1.26	0.86 (0.03)	0.968 (0.008)	106 (90)

[a] The numbers in parentheses represent the standard deviation. [b] Spin–spin relaxation time of the major component. [c] Fraction of major component contributing to the NMR signal ($f_S + f_L = 1$). [d] Spin–spin relaxation time of the minor component.

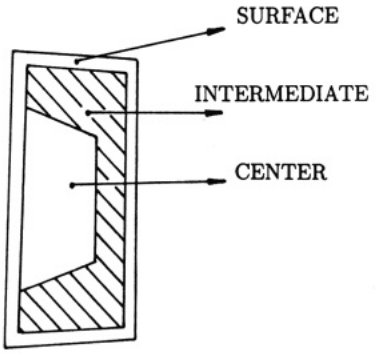

Figure 3. Sketch of an axial section of a sample representing the three regions into which the specimens were divided for destructive analysis (NMR spectroscopy and density measurements).

Results and Discussion

The ^1H NMR T_1 data were analyzed assuming the presence of only one component (a monoexponential function). No evidence was found for biexponential spin–lattice relaxation behavior. As shown in Table I, T_1 does not depend significantly on the time allowed for the hydrolysis of TEOS (an increasing amount of SiO_2). The NMR spin–lattice relaxation mechanism of the polymer is apparently not affected by the presence of small amounts of silica. T_1 is sensitive to molecular motions occurring at frequencies near the resonance frequency. In this case, the motion probably consists of reorientation of the methyl group C_3 axis by rotation of main chain segments not

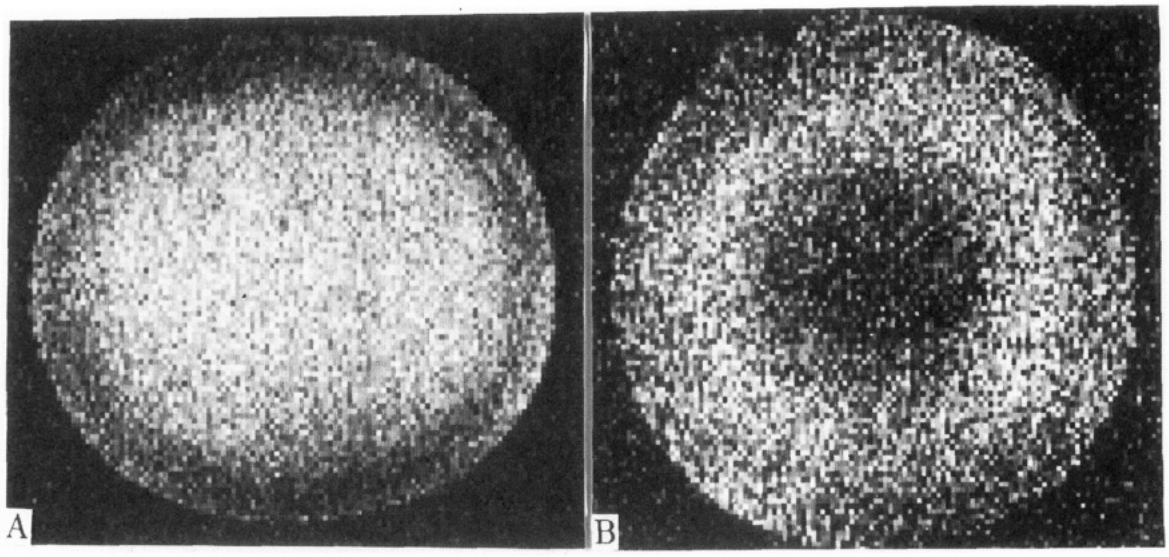

Figure 4. ^{1}H NMR images of sample 6 obtained with a two-dimensional spin-echo sequence having a TE of 3.3 (A) and 22.7 (B) ms. TR was 3 s in both cases. Selective excitation was used to define a 500-μm slice thickness in the sample transaxial plane. The resolution is 128X by 128Y pixels of 211 and 236 μm, respectively, in A and 211 μm in both axes in B. The time required to acquire the data for each image was 25.6 min. The dark rim at the edge of the sample may indicate a reduced molecular mobility of the network chains due to the presence of SiO_2.

involving many chain atoms.[26,27] The methyl group rotation about the Si–C bond is too fast at room temperature to provide an effective contribution to T_1.[26] The T_1 values obtained are similar to those of unfilled PDMS model networks with the molecular weight between cross-links, M_c, ranging from 3700 to 18 000.[28]

The analysis of the T_2 data is more complex. An apparent two-component model gives the best fit to the experimental results. The values thus obtained are shown in Table I. These data may be interpreted as the result of two contributions to the NMR signal, one from a major fraction of material attributed to the PDMS chains forming the network and the other, most likely, from the ethyl groups in partially hydrolyzed TEOS. The T_2 values of the major component agree very well with the results obtained for unfilled PDMS model networks.[28] The T_2 of the minor component (3–4%) varies with the hydrolysis time of TEOS. It is known that the hydrolysis of TEOS and subsequent condensation of the resulting silanols depend mainly on the catalyst used (acid or base) and the water content. In particular, TEOS tends to form cyclic oligomers and weakly cross-linked polymeric chains when the hydrolysis reaction is catalyzed by acids or at low water concentrations.[29] Additionally, it has been found that reesterification (the reverse of hydrolysis) plays an important role in gels prepared from acidic solutions. Therefore, it is possible to have TEOS polymer (linear, cyclic, network) with ethoxyl and hydroxyl side groups in various proportions. At the beginning of the reaction, there is a relatively high concentration of cyclic and linear oligomers. As the process evolves, increasing numbers of TEOS monomeric units are incorporated into the primary molecular structures growing into a three-dimensional network (see Figure 1). Thus, an increase in molecular rigidity might be expected and, therefore, a reduction in the T_2 of the protons in the remaining ethoxyl and hydroxyl groups. Indeed, the experimental results show an initial decrease in T_2 of the minor component, but, as the hydrolysis time increases (see Table I), the T_2s reach a plateau, before rising again at the longest hydrolysis times. The reason for the rise at long hydrolysis times may be the various competing reactions that are taking place in a highly heterogeneous process throughout the sample. This is confirmed by the NMR imaging and spectroscopy experiments.

Table II
Density of PDMS Reinforced with in Situ Precipitated SiO_2[a]

hydrolysis time, min	surface, g cm^{-3}	intermediate & center, g cm^{-3}
15	1.004 (0.009)	0.982 (0)
45	1.022 (0.007)	0.982 (0)
120	1.042 (0.020)	0.982 (0)

[a] Unfilled PDMS network: 0.971 g cm^{-3}. The numbers in parentheses represent the standard deviation.

The complexity of the process is clearly manifested by the ^{1}H NMR imaging experiments. Figure 4 shows two images, viewed along the longitudinal axis of a PDMS model network (sample 6 in Table I), obtained with a two-dimensional spin-echo sequence having TEs of 3.3 (A) and 22.7 (B) ms. The rest of the experimental conditions were the same for both images. From the values of the short and long T_2s and the fractions of short and long T_2 components in the specimens, about 36% (averaged over the six samples) of the total 3.3-ms image intensity arises from the short T_2 component; this total 3.3-ms image intensity represents only about 5% of the possible NMR signal available from the simple. The intensity of the 22.7-ms image arises only from the long T_2 component and represents typically 3% of the signal available from the sample.

The heterogeneity of the sample is readily apparent. The dark rim around the sample in Figure 4A may indicate the reduced mobility of the network chains in this region compared to that in the sample core because of a high concentration of SiO_2 as was confirmed later by density measurements (see Table II). The availability of water and catalyst at the sample periphery might be the reason for the observed difference. At long TE, the PDMS network chains do not contribute to the echo[28] and only material with high molecular mobility, i.e., oligomers from partial TEOS hydrolysis and unreacted PDMS, is visible in the NMR experiment. A slight change in the NMR images with short TE is observed with increasing hydrolysis time. Figure 5 shows three images (A–C) of samples 1, 4, and 5, respectively, taken with the same conditions as in Figure 4A. One edge of the sample appears increasingly bright as the reaction progresses. The reason

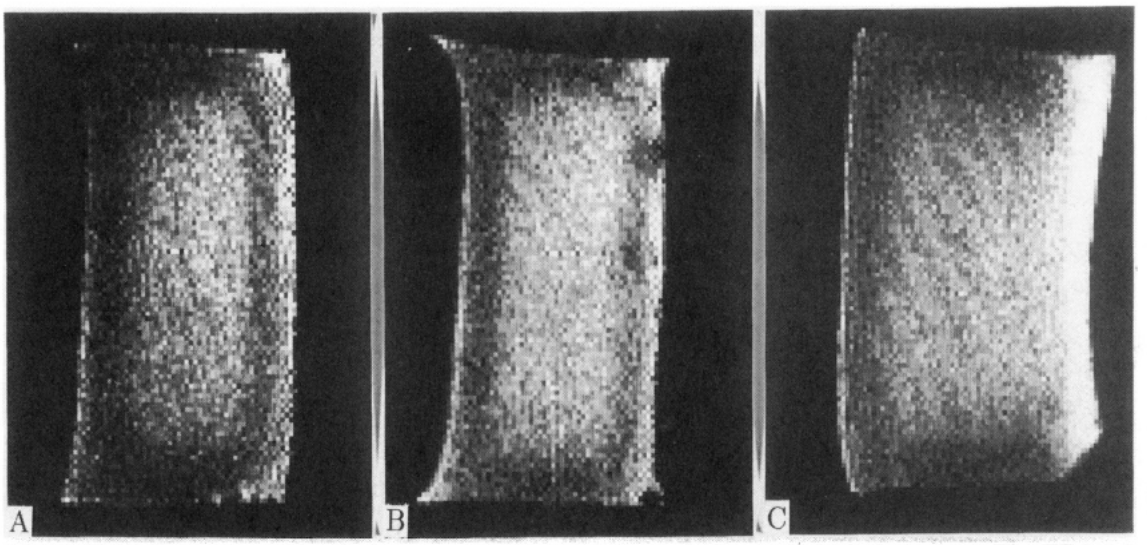

Figure 5. Axial ^1H NMR images of PDMS elastomers at (A) 15, (B) 60, and (C) 90-min hydrolysis time. The TE is 3.3 ms. The rest of the imaging parameters are similar to those in Figure 4. The resolution in these images is $128X$ by $128Y$ pixels of 185 μm in both axes. The bright edge mainly noticeable at long hydrolysis time might be due to an incomplete alkoxide hydrolysis with formation of low molecular weight materials and a weakly cross-linked SiO_2 network.

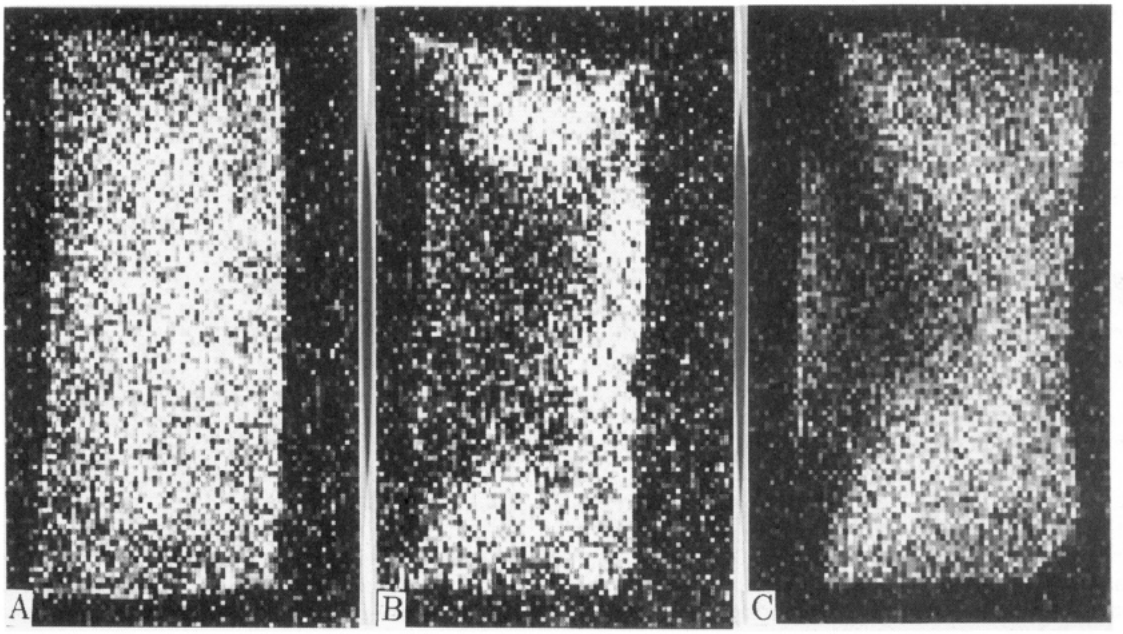

Figure 6. Axial ^1H NMR images of the samples shown in Figure 5. They were taken with the same experimental conditions as for Figure 4B. A significant variation of NMR signal intensity across the samples is observed as the hydrolysis time increases.

might be that, because of differences in density, swollen PDMS networks float in water, leaving part of them out of contact with it. In the region exposed to the air, water is less available (only atmospheric moisture), leading to an increasing presence of hydrolysis intermediates rather than SiO_2 itself.

The T_2-weighted images (long TE) show some variations of signal intensity with hydrolysis time as well. Figure 6 shows three images (A–C) of samples 1, 4, and 5, respectively, obtained with the same conditions as in Figure 4B. As mentioned above, CF_3COOH is a very efficient catalyst in promoting the TEOS hydrolysis. Therefore, changes at the edges of the sample will occur relatively rapidly, while at the center those changes are controlled by the diffusion rates of the water and catalyst in the swollen rubber. In fact, the density does not increase in the central and intermediate regions of the sample during the hydrolysis, while in the surface it changes more dramatically. These results are shown in Table II. Also, it has to be taken into account that TEOS migrates out of the sample at the same time. The later process may be responsible for the apparent distribution of low molecular weight materials as shown in the images with long echo time.

NMR spectroscopy was used to obtain chemical information on specific regions of interest in the networks as defined in Figure 3. Figure 7 shows the ^1H MAS NMR spectra of the central, intermediate, and superficial parts of sample 6 with no significant differences between them. Each spectrum is dominated by the resonance of the protons in the PDMS methyl groups at approximately 0.5 ppm. The vertical expansion of the region between 1 and 4.6 ppm shows mainly two more resonances at 1.5 and 4.0 ppm that correspond to the protons in the methyl and methylene of the ethoxyl groups, respectively.[30] These findings suggest that partially hydrolyzed TEOS is present throughout the sample. A close look at the methylene peaks also indicates some variations in their chemical shifts, perhaps a consequence of different degrees of alkoxyl substitution.[30]

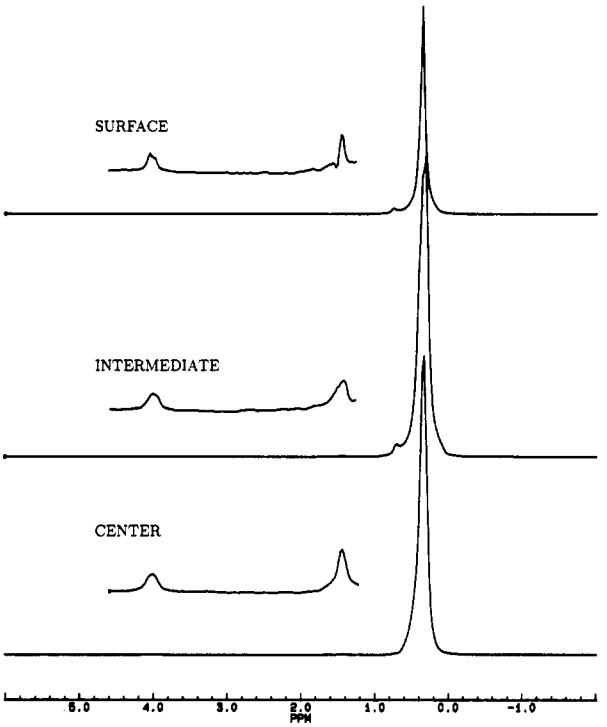

Figure 7. ^{1}H MAS NMR spectra corresponding to the center, intermediate, and surface regions of sample 6. Each spectrum was obtained with 500 acquisitions and a recycle delay of 3 s. The spinning rate was 4 kHz. The resonance peak at 0.5 ppm corresponds to the protons in the methyl groups of the PDMS chains. The insets show the vertical expansion of the spectra between 1 and 4.6 ppm with two main resonances at 1.5 and 4.0 ppm associated with the protons in the methyl and methylene parts of the ethoxyl groups, respectively. These peaks are observed in all regions, due to incomplete TEOS hydrolysis.

Figure 8 shows the ^{29}Si MAS NMR spectra corresponding to the three selected regions of sample 6. They were acquired by using a one-pulse sequence with a 45° tip angle and a recycle delay of 3 s. Similar results were obtained when employing a ~13° tip angle and 60-s recycle delay to avoid possible saturation of spins with long T_1. All the spectra have a resonance peak centered at −22.3 ppm. It is associated with the silicon atoms in the polymer backbone of the PDMS network.[31] The other silicons present in the network (i.e., in the cross-links) are not visible because of their lower concentration. The small peak at about −73 ppm is a spinning side band. The insets show the vertical expansion of the region between −80 and −135 ppm, in which the silica resonances will appear. It is clear that the surface and to a certain extent the intermediate regions have two more resonances, at −102 and −108 ppm, corresponding to the tri- (T) and tetrasubstituted (Q) silicons, respectively.[32] According to the nomenclature used in ref 32, the T and Q types are defined as a silicon atom having substituted three or four alkoxyl groups, respectively. These resonances indicate the presence of a silica network resulting from the hydrolysis and cocondensation of TEOS. With extensive averaging, the signal-to-noise ratio improves substantially, and it becomes possible to distinguish what appears as two components in the T and Q region of the spectrum (see Figure 9). The narrow peaks may be assigned to the mobile fractions of T and Q types of silicon as well as to rigid components, for which the MAS conditions used in these experiments allow the averaging of the chemical shift anisotropy. The broad components could represent fractions with motions on the order of the 4-kHz spinning frequency. In this case, the chemical shift anisotropy is not averaging out completely, resulting in a broad distribution of resonance frequencies. Alternatively, the broad components could be due to the presence of large amounts of variously substituted tri- and tetracyclic oligomers exhibiting a broad distribution of isotropic chemical shifts.

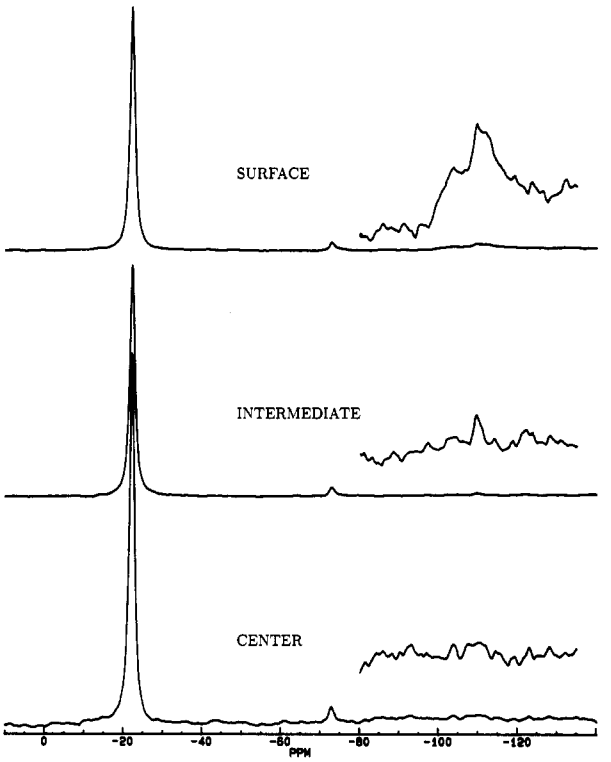

Figure 8. ^{29}Si MAS NMR spectra corresponding to various regions of the sample specified in Figure 7: center, intermediate, and surface. Each spectrum was obtained with 400 averages, a 3-s recycle delay, and a line broadening of 100 Hz. The resonance at −22.3 ppm corresponds to the silicons in the PDMS polymer backbone. The peak at about −73 ppm is a spinning side band. The insets show the vertical expansion of spectra in the region that is associated with the tri- and tetrasubstituted silicons at −102 and −108 ppm, respectively. Only at the surface is the presence of silica noticeable.

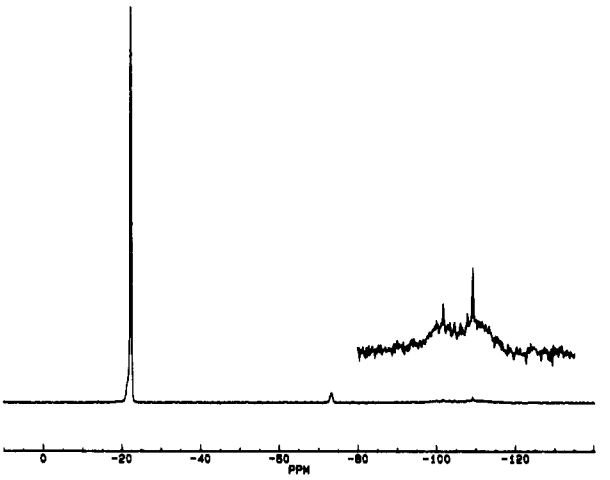

Figure 9. ^{29}Si MAS NMR spectrum of the sample 6 surface. There were 3200 acquisitions with a 3-s recycle delay, and line broadening was not applied. The line shape of the resonances corresponding to the tri- and tetrasubstituted silicons indicates the presence of two components with different degrees of molecular mobility or order.

Conclusions

These results demonstrate that proton magnetic reso-

nance imaging is capable of revealing inhomogeneities in in situ precipitated SiO_2-filled PDMS networks when relatively short reaction times and thick sections are employed. The contrast between different regions is highlighted with proton density and T_2-weighted imaging pulse sequences, suggesting that the underlying variations seen in the images may be closely related to variations in both the concentration and the mobility of the network segments. The reduced signal intensity at the sample periphery seen in proton density images indicates the presence of SiO_2. The silica network hinders molecular motion of the PDMS chains, shortening their T_2s. On the other hand, the bright edge observed in those images, particularly at long hydrolysis times, might be attributed to the ethyl groups in a more loosely cross-linked SiO_2 network.

Imaging sequences with longer echo times (T_2-weighted) show only highly mobile material that most probably is not part of the three-dimensional structure.

The NMR imaging findings are confirmed by the specific gravity measurements and the NMR spectroscopy results. It should be mentioned that only a small fraction of the total amount of protons present in the sample is visible at the conditions used in the NMR imaging experiments. When the echo time is 3.3 ms, the fraction of protons observed is ~5%, and at long echo times, it is 2–3%. In this particular situation, the quantitation of individual populations of protons (short and long T_2) is poor from image data. Solid-state imaging techniques, which are capable of imaging materials with short T_2, are in development in a number of laboratories. In the future, these imaging techniques might allow a quantitative analysis of the more rigid components in polymers. Nevertheless, it is clear that NMR imaging is extremely useful as a nondestructive tool for monitoring the uniformity of these and other synthetic materials and for learning about the details of spatially varying chemistry.

Acknowledgment. This work was supported in part by the MGH NMR Center, NIH Grant RR03264, and NSF Grant DMR 89-18002. The authors thank J. R. Moore for conducting some ^{29}Si NMR experiments.

References and Notes

(1) Rigbi, Z. *Adv. Polym. Sci.* **1980**, *36*, 21.
(2) Warrick, E. L.; Pierce, O. R.; Polmanteer, K. E.; Saam, J. C. *Rubber Chem. Technol.* **1979**, *52*, 437.
(3) Boonstra, B. B. *Polymer* **1979**, *20*, 691.
(4) Mark, J. E.; Pan, S.-J. *Makromol. Chem., Rapid Commun.* **1982**, *3*, 681.
(5) Ning, Y.-P.; Tang, M.-Y.; Jiang, C.-Y.; Mark, J. E.; Roth, W. C. *Appl. Polym. Sci.* **1984**, *29*, 3209.
(6) Jiang, C.-Y.; Mark, J. E. *Makromol. Chem.* **1984**, *185*, 2609.
(7) Jiang, C.-Y.; Mark, J. E. *Colloid Polym. Sci.* **1984**, *262*, 758.
(8) Ning, Y.-P.; Mark, J. E. *Polym. Eng. Sci.* **1986**, *26*, 167.
(9) Sun, C.-C.; Mark, J. E. *J. Polym. Sci., Polym. Phys. Ed.* **1987**, *25*, 1561.
(10) Clarson, S. J.; Mark, J. E. *Polym. Commun.* **1987**, *28*, 249.
(11) Mark, J. E.; Ning, Y.-P.; Jiang, C.-Y.; Tang, M.-Y.; Roth, W. C. *Polymer* **1985**, *26*, 2069.
(12) Mansfield, P.; Grannell, P. K. *Phys. Rev. B* **1975**, *12*, 3618.
(13) Wind, R. A.; Yannoni, C. S. *J. Magn. Reson.* **1979**, *36*, 269.
(14) Chingas, C. G.; Miller, J. B.; Garroway, A. N. *J. Magn. Reson.* **1986**, *66*, 530.
(15) De Luca, F.; Maraviglia, B. *J. Magn. Reson.* **1986**, *67*, 169.
(16) Suits, B. H.; White, D. *Solid State Commun.* **1984**, *50*, 291.
(17) Ackerman, J. L.; Garrido, L. *Seventh Annual Meeting, Society of Magnetic Resonance in Medicine*; San Francisco, CA, August 22–26, 1988; p 195.
(18) Moore, J. R.; Garrido, L.; Ackerman, J. L. *Ceram. Eng. Sci. Proc.* **1990**, *11*, 1302.
(19) Garroway, A. N.; Baum, J.; Munowitz, M. G.; Pines, A. *J. Magn. Reson.* **1984**, *60*, 337.
(20) Cory, D. G.; van Os, J. W. M.; Veeman, W. S. *J. Magn. Reson.* **1988**, *76*, 543.
(21) Szeverenyi, N. M.; Maciel, G. *J. Magn. Reson.* **1984**, *60*, 460.
(22) Emid, J.; Creyghton, J. H. N. *Phys. B* **1985**, *128*, 81.
(23) McDonald, P. J.; Attard, J. J.; Taylor, S. D. *J. Magn. Reson.* **1987**, *72*, 224.
(24) Garrido, L.; Ackerman, J. L.; Ellingson, W. A. *J. Magn. Reson.* **1990**, *88*, 340.
(25) Mark, J. E.; Sullivan, J. L. *J. Chem. Phys.* **1977**, *66*, 1006.
(26) Powles, J. G.; Hartland, A.; Kail, J. A. E. *J. Polym. Sci.* **1961**, *55*, 361.
(27) Cuniberti, C. *J. Polym. Sci., Polym. Phys. Ed.* **1970**, *8*, 2051.
(28) Garrido, L., unpublished material.
(29) Keefer, K. D. *Mater. Res. Soc. Proc.* **1984**, *32*, 15.
(30) Brinker, C. J.; Keefer, K. D.; Schaefer, D. W.; Assink, R. A. *J. Non-Cryst. Solids* **1984**, *63*, 45.
(31) Beshah, K.; Mark, J. E.; Ackerman, J. L. *J. Polym. Sci., Polym. Phys. Ed.* **1986**, *24*, 1207.
(32) Kelts, L. W.; Effinger, N. J.; Melpolder, S. M. *J. Non-Cryst. Solids* **1986**, *83*, 353.

Registry No. SiO_2, 7631-86-9.